



Universiteit  
Leiden  
The Netherlands

## Genetic dependencies in hereditary and sporadic melanoma

Christodoulou, E.

### Citation

Christodoulou, E. (2020, August 26). *Genetic dependencies in hereditary and sporadic melanoma*. Retrieved from <https://hdl.handle.net/1887/136021>

Version: Publisher's Version

License: [Licence agreement concerning inclusion of doctoral thesis in the Institutional Repository of the University of Leiden](#)

Downloaded from: <https://hdl.handle.net/1887/136021>

**Note:** To cite this publication please use the final published version (if applicable).

Cover Page



Universiteit Leiden



The handle <http://hdl.handle.net/1887/136021> holds various files of this Leiden University dissertation.

**Author:** Christodoulou, E.

**Title:** Genetic dependencies in hereditary and sporadic melanoma

**Issue date:** 2020-08-26

# Chapter 2

---

## ***NEK11* as a candidate high-penetrance melanoma susceptibility gene**

*J Med Genet.* 2020 Mar;57(3):203-210.

---

Christodoulou, E., van Doorn R., Visser, M., Teunisse, A.F.A.S., Versluis, M., van der Velden, P.A., Hayward, N., Jochemsen, A.G., Gruis, N.A.

## ABSTRACT

A proportion of patients diagnosed with cutaneous melanoma reports a positive family history. Inherited variants in *CDKN2A* and several other genes have been shown to predispose to melanoma; however, the genetic basis of familial melanoma remains unknown in most cases. The objective of this study was to provide insight into the genetic basis of familial melanoma. In order to identify novel melanoma susceptibility genes, whole exome sequencing (WES) analysis was applied in a Dutch family with melanoma. The causality of a candidate variant was characterized by performing co-segregation analysis in five affected family members using patient-derived tissues and digital PCR analysis to accurately quantify mutant allele frequency. Functional in-vitro studies were performed to assess the pathogenicity of the candidate variant. Application of WES identified a rare, nonsense variant in the *NEK11* gene (c.1120C>T, p.Arg374Ter), co-segregating in all five affected members of a Dutch family. *NEK11* (NIMA-Related Kinase 11) is involved in the DNA damage response, enforcing the G2/M cell cycle checkpoint. In a melanoma from a variant carrier, somatic loss of the wildtype allele of this putative tumor suppressor gene was demonstrated. Functional analyses showed that the *NEK11* p.Arg374Ter mutation results in strongly reduced expression of the truncated protein caused by proteasomal degradation. The *NEK11* p.Arg374Ter variant identified in this family leads to loss-of-function through protein instability. Collectively these findings support *NEK11* as a melanoma susceptibility gene.

## INTRODUCTION

Cutaneous melanoma is an aggressive type of skin cancer resulting from malignant transformation of melanocytes. Incidences of melanoma continue to rise steadily, with more than 230,000 cases diagnosed each year worldwide, accompanied by 55,000 deaths [1]. Ten percent of cases are found in people with familial predisposition, i.e. families with at least two first degree relatives with melanoma [2].

Several high-penetrance melanoma susceptibility genes have been identified and account for approximately 40% of melanoma families [3, 4]. The majority of these families are affected by germline mutations in *CDKN2A* [5], a key cell-cycle checkpoint regulator and first reported high-penetrance melanoma susceptibility gene [6-8]. Following *CDKN2A*, germline mutations in other genes have been linked to familial predisposition to melanoma; these include *CDK4* [9] and *BAP1* [10, 11]. Bi-allelic inactivation has been reported in tumor tissues with germline variants in *BAP1* including mesothelioma, uveal melanoma and cutaneous melanoma [12, 13] suggesting genetic analysis is an informative approach for discovering melanoma-predisposition genes. Considering the discovery of germline *MITF* variants, functional analysis revealed mutant *MITF* to have increased transcriptional activity, migration and invasion in melanoma cell lines [14, 15] suggesting that not only genetic analysis in patient's tissues but also functional validation adds to the current value of mutation screening. Application of Whole Exome Sequencing (WES) analysis has been successful in identifying rare variants including *TERT* promoter [16], *POT1* [17] *TERF2IP* and *ACD* [18], *GOLM1* [19], *EBF3* [20] and *POLE* [21] as candidate high-penetrance melanoma susceptibility genes. Still, the genetic basis of over half of melanoma families remains unknown, impairing genetic testing and counselling in families with predisposition to melanoma [22, 23]. Here, *NEK11* gene was identified by WES in a Dutch family with melanoma and characterized as a potential novel high-penetrance melanoma-susceptibility gene.

## METHODS

### Whole exome sequencing (WES)

#### *Study population and ethics approval*

WES was carried out in blood-derived DNA samples of two members of a Dutch familial melanoma family. Study approval was obtained by the ethics committee of Leiden University Medical Center (LUMC, P00.117).

#### *Sequencing analysis and bioinformatics*

Sequencing was performed on HiSeq2000 platform with TruSeq Exome Enrichment kit. Paired-end reads of 110 bp were generated with mean coverage of 40X. The Burrows-Wheeler aligner was used for mapping sequencing reads to the reference UCSC human genome. SNVs were detected using samtools/bcftools. Indels were detected with Pindel and annotated to dbSNP144 using ANNOVAR. Variants altering the coding sequence were selected excluding those that were present at a frequency of 0.0005% or higher in the Kaviar (Known VARIants) control population database, including 162 million variants from human genomes of datasets such as ExAc and 1000Gs [24].

#### *Selection, validation and interpretation of variants*

Variants identified were assessed to identify pathogenic or potentially pathogenic variants in ClinVar. Variants were then filtered using *in-silico* prediction algorithms to show if an alteration affects protein function. Details about criteria for interpretation of variants has been reported previously [25]. These included exonic, frameshift, non-synonymous SNVs, splicing and stop-gain SNVs. We then focused on segregating mutations between all family members and functional significance. Co-segregation of *NEK11* p.Arg374Ter mutation was confirmed using Sanger sequencing of germline DNA from family members 1, 4, 5, 7 and 12 (Supplemental Table 1) (Macrogen, Amsterdam, The Netherlands).

### Genotyping and LOH analysis

DNA was extracted from primary melanoma FFPE tissue of a *NEK11* p.Arg374Ter mutation carrier (family member 5) using the QIAamp DNA FFPE Tissue kit (QIAGEN, Venlo, The Netherlands) according to manufacturer's instructions. DNA extraction of normal and tumor tissue was obtained through micro-dissection/punch biopsy by the pathology department of LUMC, The Netherlands. Genomic primer sets were used to amplify the region of interest containing the mutation (*NEK11* c.1120C>T) and a common SNP (rs4974475, chr3:130882827, MAF 17%), located at 2 kb upstream from the *NEK11* mutation site to verify LOH (Supplemental Table 1). PCR products were cleaned-up using a PCR clean-up protocol (Bio-Rad, Hercules, California, USA) and sequenced by Sanger sequencing analysis-long run

(Macrogen, Amsterdam, The Netherlands). Chromatograms were then analyzed by Chromas Technelysium DNA Sequencing Software (Technelysium Pty Ltd, South Brisbane, Australia).

### Digital PCR analysis (dPCR)

Mutation detection assays specific for dPCR (Bio-Rad, Hercules, California, USA) describe the incorporation of both wild-type and mutated targets in a single dPCR mix. In this case, the assay was designed for the detection of *NEK11* p.Arg374Ter mutation. Detailed protocol of mutation detection dPCR assay has been described previously [26] and dPCR sequence information is provided in Supplemental Table 1. QuantaSoft software (Bio-Rad, Hercules, California, United States) was used to analyze the data by calculating the concentration of the amplified dPCR product (copies/ $\mu$ l) [26]. The wild-type (WT) allele frequency was calculated by dividing the WT allele counts over the total allele counts and the mutant (MT) allele frequency was calculated by dividing MT allele counts over the total allele counts.

### Cell culturing and maintenance

U2OS (human osteosarcoma tumor cell line) and FM6 (human cutaneous malignant melanoma cell line) cells were maintained in DMEM medium supplemented with penicillin (100 I.U./mL)/streptomycin (100  $\mu$ g/mL) and 10% Fetal Bovine Serum (FBS) and glutamax 100x (Thermo Fisher Scientific, Waltham, Massachusetts, United States). All cells were grown in a humidified incubator at 37°C and 5% CO<sub>2</sub> and routinely sub-cultured when reaching 95% confluency.

### Plasmid construction and introduction of *NEK11* p.Arg374Ter mutation

*NEK11*-FL (full-length isoform [27]) was expressed from a plasmid construct containing WT *NEK11* cDNA, fused with N-terminal FLAG-epitope tag (Kind gift from professor Andrew Fry, University of Leicester, UK) for expression in U2OS and FM6 cells [27]. Site-directed mutagenesis was applied to introduce *NEK11* p.Arg374Ter mutation in flag-tagged *NEK11* expression vectors. Primer-sets were designed specifically targeting the mutation site of *NEK11* exonic sequence (Supplemental Table 1). Thermal cycling was performed to introduce the mutation consisting of 1-minute denaturation at 95°C, followed by 10 cycles of 1-minute steps at 95°C, 63°C and 68°C. The PCR product was then digested with *DpnI* enzyme and transformed into Top10 bacteria to produce inducible vectors for functional experiments. Sequences of both *NEK11* WT and MT expression vectors were confirmed by Sanger Sequencing analysis long-run (Macrogen, Amsterdam, The Netherlands) (Supplemental Table 1).

## Lentivirus production

*NEK11* WT and MT cDNAs were re-cloned into a lentiviral backbone containing the neomycin resistance gene. Lentiviral stocks were produced by transfections into HEK-293T cells as described previously [28] but calcium phosphate was replaced with polyethylenimine (PEI) in the transfection mix. Virus was quantified by antigen capture enzyme-linked immunosorbent assay (ELISA) measuring HIV p24 levels (ZeptoMetrix Corp., New York, NY, USA).

## Transient transfections

U2OS cells were harvested and seeded in appropriate growth medium in 6-well plates ( $0.5 \times 10^5$  cells/ml) and 60-mm dishes ( $1.8 \times 10^5$  cells/ml). The DNA mix was prepared as follows:  $0.8 \mu\text{g}$  *pLV-NEO-NEK11-WT*, *pLV-NEO-NEK11-MT* and *pLV-NEO-empty* lentiviral vectors (see lentivirus production section),  $0.1 \mu\text{g}$  *Tomato-Red*, 300ng of *GFP* expression vector and  $0.2 \mu\text{g}$  *pSuper*. The PEI mix was prepared as follows: 3:1 PEI (3 parts of PEI to 1 part of DNA concentration) diluted in Gibco™ Opti-MEM™ Reduced Serum medium (Thermo Fisher Scientific, Waltham, Massachusetts, United States). PEI mix was added slowly to DNA mix followed by a short vortex. The mixture was kept at RT for 20 minutes and then added dropwise to U2OS cells. Growth medium was replaced 16 hours after transfection and U2OS cells were further incubated for another 24 hours.

## Lentiviral transductions

Fresh culture media were prepared with viral supernatants supplemented with  $8 \mu\text{g/ml}$  polybrene (Sigma-Aldrich, St. Louis, Missouri, United States). FM6 cells were seeded in 6-well plates at a density of  $2 \times 10^5$  cells/well. FM6 cells were incubated with virus-containing medium overnight, after which the cells were refed with fresh medium containing G418 (Sigma-Aldrich, St. Louis, Missouri, United States) to produce stable cell lines expressing *NEK11* WT and MT by using neomycin as selection marker.

## RNA isolation, cDNA synthesis and gene expression analysis

Lymphocytic RNA of a *NEK11* p.Arg374Ter carrier (family member 18) and a non-relative spouse was isolated using the RNeasy micro kit from QIAGEN (Venlo, The Netherlands). RNA was isolated from FM6 cells using the SV total RNA isolation kit (Promega, Fitchburg, WI, USA). First strand cDNA synthesis was carried out using the iScript™ c-DNA synthesis kit (Bio-Rad, Hercules, California, USA) and Sanger Sequencing analysis (LGTC, LUMC, The Netherlands) was used to detect presence of *NEK11* WT and MT alleles (Primer sequences shown at Supplemental Table 1). *NEK11* gene expression was confirmed using SYBR® green based quantitative PCR on CFX384 Touch Real-Time PCR Detection System (Bio-Rad, Hercules, California, USA) (Supplemental Table 1). Gene expression results were analyzed using Bio-Rad CFX Manager 3.1 Software (Hercules, California, USA) and corrected relative to



reference gene expression (*CAPNS1* and *SRPR*) as well as transfection efficiency target *Tomato-Red* (Supplemental Table 1).

### Immunofluorescence staining

Transfected U2OS cells on cover slips were washed twice in phosphate-buffered saline (PBS) solution and fixed with 4% paraformaldehyde (PFA) for 10 minutes. Cover slips with U2OS cells were then incubated for 10 minutes in PBS/0.2%Triton-X100 (permeabilization) and pre-incubated for 30 minutes in PBS/0.05% Tween-20 containing 5% normal goat serum (NGS). Subsequently, U2OS cells were incubated with monoclonal anti-flag M2 Catalog Number F1804 (Sigma-Aldrich, St. Louis, Missouri, United States) diluted in PBS/Tween/NGS (1:500) for 60 minutes at room temperature followed by washing three times in PBS/Tween for a total of 15 minutes. The secondary antibody, anti-Mouse IgG-Cy2 (#115-225-146, Jackson ImmunoResearch Laboratories, Cambridge, UK) was diluted in PBS/Tween/NGS (1:100) and added at room temperature in the dark. U2OS cells were finally washed for 10 minutes with PBS/Tween and coverslips were placed on slides for analysis on a Leica DMRA fluorescent microscope (Nijmegen, The Netherlands).

### Drug Treatments

MG132 proteasome inhibitor (Sigma-Aldrich, St. Louis, Missouri, United States) was added to U2OS and FM6 cells at a final concentration of 20  $\mu$ M for 5-6 hours before RNA and protein isolation procedures. The cycloheximide (CHX), translation inhibitor, was added at a concentration of 50  $\mu$ g/ml (Sigma-Aldrich, St. Louis, Missouri, United States) to FM6 stable-cell lines expressing *NEK11* WT and *NEK11* MT as a time-course treatment of 0, 1, 2 and 4 hours.

### Protein isolation and Western Immunoblotting analysis

U2OS and FM6 cells were washed twice in ice-cold PBS and incubated on ice for 10 minutes in Giordano buffer (50mM Tris-HCl pH7.4, 250mM NaCl, 0.1% Triton X-100 and 5mM EDTA; supplemented with phosphatase and protease inhibitors). Lysates were collected by scraping and centrifuged at max speed for 10 minutes and protein concentration was determined using the Bradford method. Western Blot procedure was followed as described previously [29]. *NEK11* protein was detected by the Anti-Flag antibody (1:1000) (Sigma-Aldrich, St. Louis, Missouri, United States) and the controls were detected by Anti-USP7 (1:1000) (Bethyl Laboratories, Biomol, Montgomery, Texas, USA), Anti-GAPDH (1:1000) (Sigma-Aldrich, St. Louis, Missouri, United States) and Anti-P53 (1:1000) (Santa Cruz Biotechnology, Heidelberg, Germany). After transient expression, protein levels were determined using the Odyssey machine (LI-COR, Lincoln, Nebraska, United States) and analyzed using Odyssey software according to manufacturer's instructions. Secondary antibodies used were IRDye® 800CW Goat anti-Mouse IgG (H + L), 0.1 mg (1:5000) and IRDye® 680LT Goat anti-Rabbit IgG (H + L), 0.1 mg (1:5000)

(LI-COR, Lincoln, NE, United States). Due to low protein expression in stably-transduced FM6 cells, the ChemiDoc Imaging System was used to detect proteins with increased sensitivity and specificity. The bands were analyzed with Image lab software (Bio-Rad, Hercules, California, USA) according to manufacturer's instructions. Protein-expression quantification was performed relative to unaffected expression of controls (GAPDH, USP7).

### **Statistical Analysis**

All data were analyzed by calculating the mean and standard deviation (SD) and graphs were obtained in GraphPad Prism version 7 (GraphPad software, San Diego, CA, USA). ANOVA and multiple comparisons were applied to detect statistically significant differences between expression patterns of three independent experiments (n=3). Statistical significance was reached when  $p < 0.05$ .

## RESULTS

### WES analysis and identification of *NEK11* p.Arg374Ter

A Dutch melanoma family presented four melanoma cases and one uveal melanoma case with prostate cancer. The diagnosis of melanoma in five members in multiple generations strongly suggests an autosomal dominant mode of inheritance (Figure 1) and members were negative for mutations in established melanoma susceptibility genes (*CDKN2A*, *BAP1*, *POT1*, *TERT*, *TERF2IP*, *ACD*, *MITE*, *GOLM1*, *EBF3*). A WES analysis was carried out on DNA from blood cells of two affected members (Figure 1). Among a total of 19 rare, co-segregating non-synonymous variants that met our criteria, 17 were missense mutations, probably damaging, predicted deleterious [30, 31]. These variants however, are not plausible candidate melanoma susceptibility genes (Table 1) since there is no evidence supporting a strong tumorigenic effect based on published literature. Interestingly, two were nonsense stop-gain single nucleotide variants (SNVs) (Table 1). One candidate stop-gain variant was p.Arg66Ter in *ZNF192*, a gene possibly regulating transcription. However, no implications in cancer have been mentioned in published literature. In contrast, the other candidate was a truncating variant (p.Arg374Ter) in the never in mitosis-gene A (NIMA)-related kinase 11 (*NEK11*). This family of proteins functions in different aspects of cell cycle regulation, although the in-depth role of NIMA-related kinases remains to be uncovered [32]. *NEK11* has been reported to be somatically mutated in different types of cancer, including lung, breast, prostate and melanoma [33]. The frequency of *NEK11* mutations was >5% in melanomas [34, 35] suggesting a plausible candidate in melanoma development.

Sanger sequencing confirmed *NEK11* p.Arg374Ter to co-segregate within four cutaneous melanoma cases and one uveal melanoma case in this Dutch melanoma family (Figure 1). Family members 13 and 16 were also found to be *NEK11* p.Arg374Ter carriers although with no clinical presentation of cancer/melanoma. Considering the current age of these individuals and absence of the melanoma phenotype, the possibility for non-penetrance is very likely (Figure 1). Somatic loss of the wildtype (WT) allele was detected in primary cutaneous melanoma tissue of a mutation carrier (Figure 2A-C) and confirmed by the highly sensitive and quantitative method, digital PCR (dPCR) [36] whereby, a higher fraction of *NEK11* p.Arg374Ter mutant (MT) than *NEK11* WT allele was detected in melanoma tissue when compared to normal tissue micro dissected from the same biopsy sample (Figure 2D). Furthermore, examination of a common SNP (rs4974475, chr3:130882827, MAF 17%), showed loss of this variant in the melanoma tissue of a *NEK11* p.Arg374Ter carrier, suggesting LOH over a longer genetic region (Supplemental Figure 1). Collectively, these data suggest a potential loss-of-function (LOF) mutagenic effect of *NEK11* p.Arg374Ter.

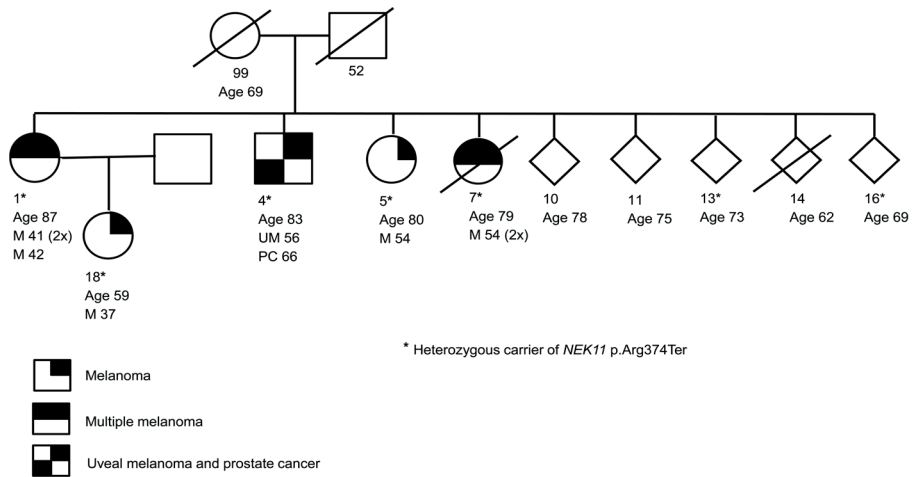


**Figure 1 Co-segregation of *NEK11* p.Arg374Ter in a Dutch melanoma family.** Whole-exome sequencing was carried out for family members 1 and 4. Co-segregation of *NEK11* p.Arg374Ter was confirmed by analyzing germline DNA from all family members. Current age and age at death of deceased individuals (those reported) are indicated. Age at diagnosis of each tumor type is noted in affected family members (M = melanoma, UM= uveal melanoma, PC= prostate cancer).

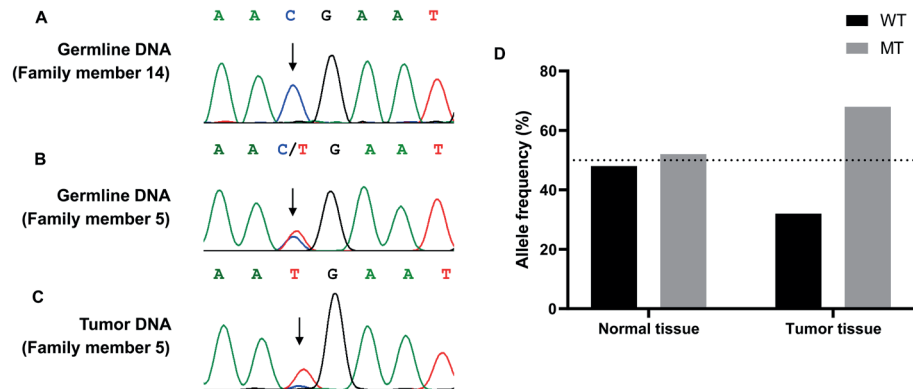


**Figure 2 LOH analysis of a *NEK11* p.Arg374Ter mutation carrier.** Chromatogram showing DNA sequence of **A**) healthy family member (14), **B**) a *NEK11* p.Arg374Ter carrier (family member 5) and **C**) tumor of a *NEK11* p.Arg374Ter carrier (family member 5). Arrows indicate the *NEK11* p.Arg374Ter mutation site. **D**) dPCR *NEK11* mutation assay showing the *NEK11* wildtype (WT) and *NEK11* p.Arg374Ter (MT) allele frequency detected in normal and tumor tissue from FFPE derived DNA of family member 5.

**Table 1 Summary of Whole-exome sequencing (WES) analysis and identification of segregating novel predicted damaging/deleterious variants in a Dutch melanoma family.**

Gene	Change	Ch	Ref	Alt	Type <sup>a</sup>	SIFT	Polyphen	MAF <sup>b</sup>
<i>GPATCH3</i>	p.Gly131Arg	1	C	T	missense	deleterious	probably_damaging	0.00006168
<i>ATPIF1</i>	p.Arg94His	1	G	A	missense	deleterious	probably_damaging	0.00004406
<i>KALRN</i>	p.Ser1629Cys	3	C	G	missense	deleterious	probably_damaging	0.00002641
<i>NEK11</i>	p.Arg374Ter	3	C	T	stop-gained			0.00002641
<i>ZNF192</i>	p.Arg66Ter	6	C	T	stop-gained			0.000008791
<i>GPR111</i>	p.Ser168Arg	6	T	A	missense	deleterious	probably_damaging	0.00006486
<i>GPAM</i>	p.Pro403Thr	10	G	T	missense	deleterious	probably_damaging	0.000008794
<i>NELL1</i>	p.Val755Met	11	G	A	missense	deleterious	probably_damaging	0.0002261
<i>KRT77</i>	p.Asp316Asn	12	C	T	missense	deleterious	probably_damaging	0.00001502
<i>OAS2</i>	p.Tyr269Cys	12	A	G	missense	deleterious	probably_damaging	-
<i>DNAJC3</i>	p.Arg346Gln	13	G	A	missense	deleterious	probably_damaging	0.0001553
<i>TEP1</i>	p.Arg1386Trp	14	G	A	missense	deleterious	possibly_damaging	0.001266
<i>PLCB2</i>	p.Arg253Trp	15	G	A	missense	deleterious	probably_damaging	0.001074
<i>DNASE1</i>	p.Ala168Val	16	C	T	missense	deleterious	possibly_damaging	0.001402
<i>BFAR</i>	p.Phe53Ile	16	T	A	missense	deleterious	possibly_damaging	-
<i>ITGB4</i>	p.Arg556Cys	17	C	T	missense	deleterious	possibly_damaging	0.0006357
<i>PSG7</i>	p.Trp67Ser	19	C	G	missense	deleterious	probably_damaging	0.0001473
<i>GPR50</i>	p.Gly93Ala	X	G	C	missense	deleterious	possibly_damaging	0.00001240
<i>GABRQ</i>	p.Arg254Cys	X	C	T	missense	deleterious	probably_damaging	0.00007713

<sup>a</sup> Variants characterized by ExAC/gnomAD/Genome of The Netherlands/Ensembl databases

<sup>b</sup> MAF in European (Non-Finnish) population

## Functional analysis of NEK11 p.Arg374Ter

Following genetic characterization of *NEK11* p.Arg374Ter as a potential LOF mutation, functional analyses were performed to investigate the effects of this truncating mutation on the expression level of *NEK11* mRNA and *NEK11* protein. Upon transient transfection of *NEK11* expressing plasmids in osteosarcoma tumor cell line U2OS the expression of *NEK11* MT mRNA was lower than *NEK11* WT mRNA, although the difference was statistically not significant (Supplemental Figure 2). U2OS cell-line provided the ideal conditions for functional analysis since it is an easily transfectable, fast-growing cell line and has been previously used to functionally characterize *NEK11* [27, 37, 38]. *NEK11* MT mRNA expression was detected in lymphocyte mRNA of a mutation carrier by Sanger sequencing and dPCR analyses (Figure 3A-C) suggesting that the premature stop codon does not result in significant transcript degradation by nonsense-mediated mRNA decay (NMD). Combined with the finding that the mutant *NEK11* mRNA was detected in U2OS cells (Supplemental Figure 2), these results indicate no significant effect of the mutation on *NEK11* mRNA expression levels.

Introduction of p.Arg374Ter mutation in the *NEK11* expression vector, resulted in synthesis of a truncated *NEK11* protein lacking the whole C-terminal PEST-like domain as well as part of the coiled-coil motifs (Supplemental Figure 3A). The coiled-coil region regulates protein activation suggesting that loss or absence of these motifs would affect protein function [39]. The truncated protein runs at approximately 45 kDa, which reasonably fits with the size of 373 amino acids (Supplemental Figure 3A). Immunoblot analysis of protein lysates made from transfected U2OS cells showed that the level of the truncated protein was 3-fold lower than *NEK11* WT expression ( $p < 0.005$ ; Figure 4A and B) when corrected for mRNA expression. Treatment with the proteasome inhibitor MG132 increased *NEK11* protein level, particularly of the truncated product (~ 2 fold). Still, the difference between *NEK11* WT and MT protein levels in lysates of MG132-treated U2OS cells is significant ( $p < 0.005$ ). Collectively, statistically significant lower protein expression was correlated with the *NEK11* p.Arg374Ter mutation.

Since a distinct subcellular localization of *NEK11*-FL (645 amino acids) and *NEK11*-S (450 amino acids) has been reported [27], which might affect the protein expression level, the subcellular localization of the Flag-tagged *NEK11* MT was investigated in comparison to Flag-tagged *NEK11*-FL. Interestingly, both proteins were mainly localized in the nucleus of U2OS cells (Supplemental Figure 3B), in contrast to the earlier publication. However, in that publication GFP-tagged constructs were used. Indeed, using the same GFP-tagged constructs the subcellular localization of *NEK11*-FL and *NEK11*-S was as reported; the GFP-*NEK11* MT protein localized in the nucleus, similar to GFP-*NEK11*-S (data not shown).

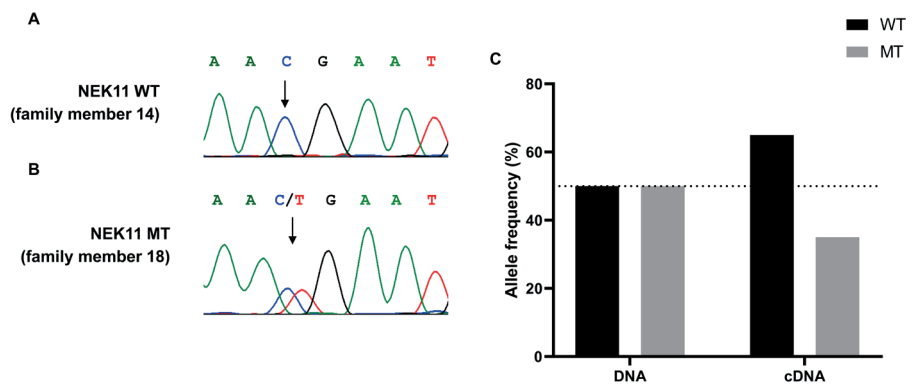


**Figure 3** *NEK11* wildtype and *NEK11* p.Arg374Ter mRNA analysis. Chromatogram showing sequence from cDNA of **A)** healthy family member 14, and **B)** a *NEK11* p.Arg374Ter carrier (family member 18) Arrows indicate the *NEK11* p.Arg374Ter mutation site. **C)** Allele frequency of *NEK11* wildtype (WT) and *NEK11* p.Arg374Ter (MT) detected by dPCR *NEK11* mutation assay using DNA and cDNA from family member 18.

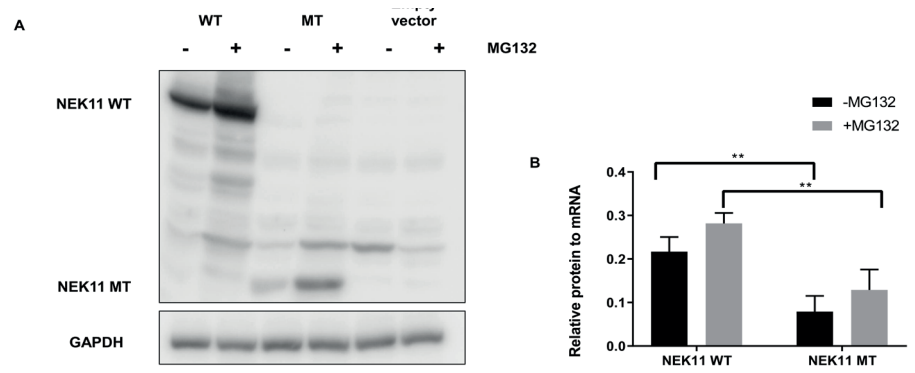


**Figure 4** Expression of *NEK11* wildtype and p.Arg374Ter in U2OS cells. **A)** Lysates of U2OS cells transiently transfected with *NEK11* wildtype (WT) , *NEK11* p.Arg374Ter (MT) and *pLV-empty* expression plasmids were either untreated or treated with MG132. *NEK11* was detected with anti-Flag antibody. GAPDH was determined as a loading control. **B)** Expression was calculated relative to GAPDH for each independent experiment and corrected for mRNA expression of *NEK11*. Data shown represent mean expression from 3 independent experiments. Error bars represent Standard Deviation (SD). Statistical significance is shown as \* $p < 0.05$ , \*\* $p < 0.005$ .

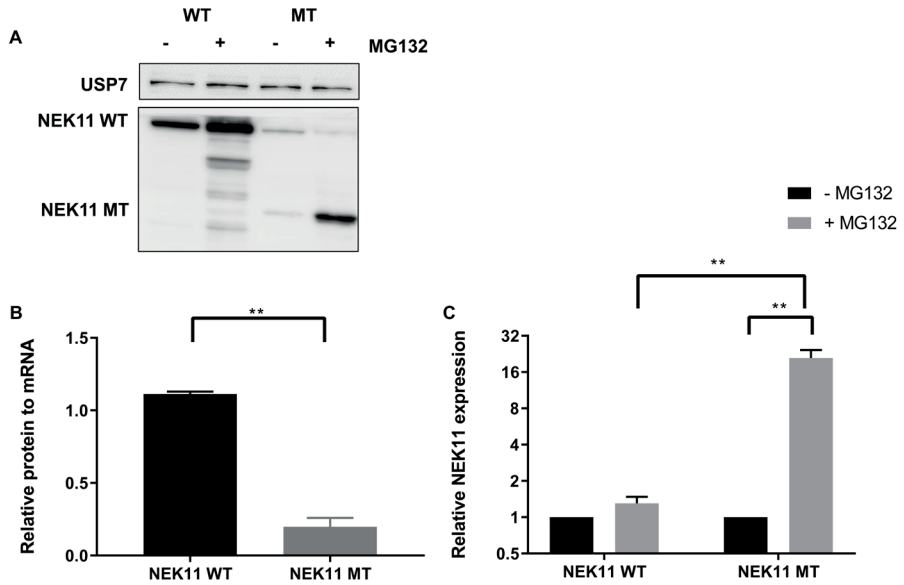


**Figure 5 NEK11 protein expression and quantification in stably-transduced FM6 cells.** **A)** Western blot analysis of cell lysates extracted from stably transduced FM6 cells, either untreated or treated with MG132. NEK11 was detected using anti-Flag antibody. USP7 was detected as a loading control. **B)** Protein expression quantifications. Expression was calculated relative to USP7 for each independent experiment and corrected for mRNA expression. **C)** Effect of MG132 on NEK11 wildtype (WT) and p.Arg374Ter (MT) expression. NEK11 WT and MT expression was set to 1 and the log<sub>10</sub> relative expression to USP7 is shown. Unpaired t-test was performed for statistical significance. Experiments performed in duplicates. Error bars represent Standard Deviation (SD). Statistical significance is shown as \*p<0.05, \*\*p<0.005.



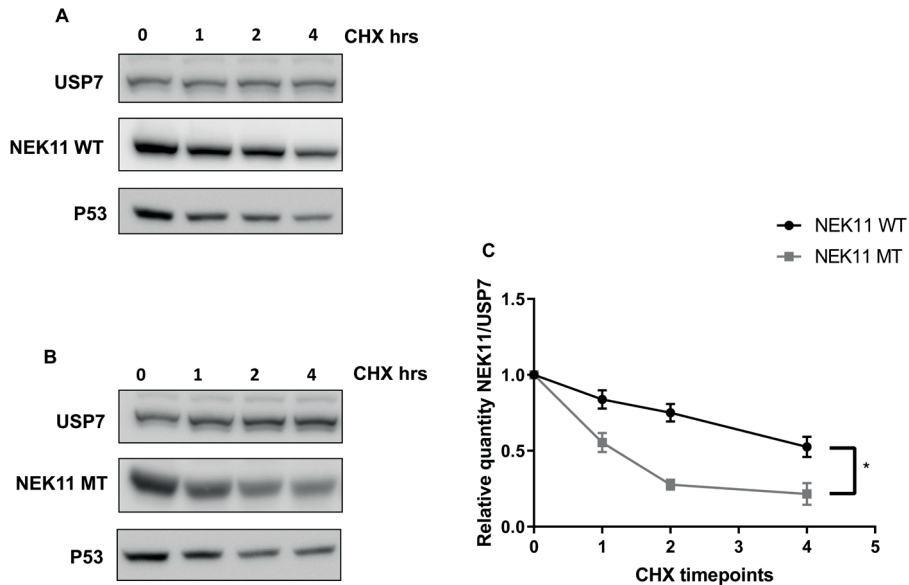


**Figure 6** NEK11 protein half-life analysis in FM6 cells using cycloheximide (CHX) treatments. Time-course CHX treatments of FM6 cells expressing **A)** NEK11 wildtype (WT) and **B)** NEK11 p.Arg374Ter (MT). USP7 was detected as a loading control and P53 as a positive control. **C)** Quantification of NEK11 WT and MT corrected for USP7 expression over different time-points of CHX treatments. Error bars represent Standard Deviation (SD). Pearson R squared correlation value was 0.82. Statistical significance is shown as \* $p < 0.05$ , \*\* $p < 0.005$ , \*\*\* $p < 0.0005$ .

Since transient overexpression yields very high expression levels which might partly mask normal regulation of NEK11 protein expression, a putative difference in protein expression of the NEK11 WT and the NEK11 MT was studied in more detail in stably-transduced, disease-relevant FM6 cutaneous melanoma cells. Strikingly, NEK11 MT protein expression was hardly detectable with 6-fold difference compared to NEK11 WT when corrected to mRNA levels ( $p = 0.0024$ ) (Figure 5A and B). Furthermore, treating FM6 cells with MG132 strongly increased NEK11 MT protein level (Figure 5C), while the effect of MG132 on NEK11 WT levels was much less pronounced, suggesting that the truncated NEK11 protein is prone to faster protein degradation. To examine protein half-life of the NEK11 WT and MT proteins, we decided to treat these FM6 cells with the protein translation inhibitor cycloheximide (CHX) and harvest at different time-points. The NEK11 WT protein appeared to be a stably expressed protein with half-life of approximately 4 hours, in contrast to the NEK11 MT protein showing a half-life of approximately 1 hour in FM6 cells (Figure 6A-C). Collectively, we provide evidence that the *NEK11* p.Arg374Ter mutation leads to the synthesis of a truncated protein with a very short half-life, suggesting a LOF mutation, supporting a tumor-suppressive role for *NEK11* in familial melanoma.

## DISCUSSION

Here, a novel nonsense protein truncating variant in *NEK11* p.Arg374Ter was identified as a possible familial melanoma predisposition mutation in a Dutch family. The possibility of any other potentially damaging variants found by WES in this family to either be causal or contributing to the melanoma-risk of this family was considered. Since not enough scientific evidence was available to support a contributing role, these variants were not investigated further.

*NEK11* has been initially characterized as a DNA-damage response kinase with two isoforms, the full-length isoform consisting of 645 residues (*NEK11-FL*) and the short isoform consisting of 470 residues (*NEK11-S*) [37]. A regulatory effect during IR-induced G2/M cell-cycle arrest has been described, i.e. *NEK11* was shown to be involved in phosphorylation of *CDC25A* triggering its degradation and ultimate blocking of progression into mitosis [27, 38, 40]. *NEK11* has been described to (de) regulate G2/M cell-cycle arrest in colorectal carcinoma and low expression was observed at late-advanced stages of the disease [27, 40]. Furthermore, decreased *NEK11* mRNA levels have also been associated with drug resistance in ovarian cancer cells [41] supporting that *NEK11* may prevent metastatic progression in ovarian cancer. Collectively, these results point towards a putative tumor suppressive role of *NEK11*.

*NEK11* expression follows a cell-cycle dependent manner with a peak at G2/M phase [38] and mRNA expression is found in the brain, uterus and lungs with moderate expression in melanoma (median expression = 6) [42, 43]. No significant difference in expression between benign nevi and melanomas can be observed [34], however, cutaneous melanoma patients with higher *NEK11* expression have slightly improved survival, although this association is not statistically significant [44]. Moreover, *NEK11* has been suggested to play a role in the G1/S checkpoint in association with *NEK2*, however, the exact mechanism remains unknown [39, 45]. Therefore, these data suggest that *NEK11* could be regarded an interesting target to validate as a high-penetrance melanoma susceptibility gene.

Genetic analysis confirmed LOH in the melanoma tissue of a mutation carrier. Expression of *NEK11* MT and *NEK11* WT allele is detected in lymphocytic RNA indicating that the mutant transcript is not degraded by NMD, confirmed by mRNA expression analysis in transfected U2OS cells.

The oncogenicity of the *NEK11* p.Arg374Ter mutation could be caused by two possible scenarios. First, a gain-of-function (GOF) mutation, as the non-catalytic C-terminal domain was shown to have an auto-inhibitory effect on protein function [45], thus, loss of this domain could activate the kinase activity. Alternatively, the mutation might lead to the synthesis of a non-functional truncated protein, e.g.

by loss of coiled-coil domain motifs (Supplemental Figure 3A). Here, we provide data strongly suggesting a LOF of the *NEK11* p.Arg374Ter mutation. Collectively our results implicate that the truncated *NEK11* protein has a very short half-life, implying that the mutant protein is not significantly expressed in cells and reflects a loss-of-function. Since loss of *NEK11* abrogates the G2/M cell cycle arrest upon DNA damaging agents and can induce apoptosis [25], it is very well possible that LOF results in genomic instability with the possible selection of cells with increased survival and proliferation, stimulating the acquirement of additional mutations and the development into a tumor.

Unfortunately, our analyses of *NEK11* p.Arg374Ter mutation were restricted by the limited availability of relevant (tumor) tissue, as we only had access to melanoma tissue and lymphocytic RNA from one affected family member. Analysis of tumor tissue from more affected family members could strengthen the case for *NEK11* as a novel melanoma-susceptibility gene. Moreover, the *NEK11* p.Arg374Ter mutation had 14 submissions in dbSNP, although frequency of the alternate allele was extremely low (0-0.00003) and was not found in the Genome of The Netherlands (GoNL) database [30, 46, 47]. In a recent study, >300.000 UK WES/WGS non-melanoma data sets were analyzed for non-synonymous protein truncating variants (PTVs) [48], however, no mutations were identified in *NEK11*, further strengthening *NEK11* to be a novel but rare melanoma-susceptibility gene and p.Arg374Ter as a potential pathogenic mutation.

As to why this family is predisposed to develop melanoma and not a different tumor type, we cannot conclude based on data from a single family. The increased risk of only one or a few tumor types is common in monogenic tumor predisposition syndromes [49]. Furthermore, the absence of any *NEK11* mutation in 488 Dutch familial melanoma cases [50] warrants screening for *NEK11* mutations in melanoma families worldwide in order to confirm the importance of *NEK11* as a melanoma-susceptibility gene.

## ACKNOWLEDGEMENTS

This project has received funding from the European Union's Horizon 2020 research and innovation programme under grant agreement No 641458. Mijke Visser and Nick Hayward were supported by grant from the Dutch Cancer Society (UL2012-5489) and the National Health and Medical Research Council of Australia, respectively.

## REFERENCES

1. Schadendorf, D., A.C.J. van Akkooi, C. Berking, K.G. Griewank, R. Gutzmer, A. Hauschild, et al., Melanoma. *The Lancet*, 2018. **392**(10151): p. 971-984.
2. Leachman, S.A., J. Carucci, W. Kohlmann, K.C. Banks, M.M. Asgari, W. Bergman, et al., Selection criteria for genetic assessment of patients with familial melanoma. *Journal of American Academy of Dermatology*, 2009. **61**(4): p. 677.e1-14.
3. Potrony, M., C. Badenas, P. Aguilera, J.A. Puig-Butille, C. Carrera, J. Malvehy, et al., Update in genetic susceptibility in melanoma. *Annals of Translational Medicine*, 2015. **3**(15).
4. Aoude, L.G., K.A. Wadt, A.L. Pritchard, and N.K. Hayward, Genetics of familial melanoma: 20 years after CDKN2A. *Pigment Cell Melanoma Research*, 2015. **28**(2): p. 148-60.
5. Goldstein, A.M., M. Chan, M. Harland, N.K. Hayward, F. Demenais, D.T. Bishop, et al., Features associated with germline CDKN2A mutations: a GenoMEL study of melanoma-prone families from three continents. *Journal of Medical Genetics*, 2007. **44**(2): p. 99-106.
6. Kamb, A., D. Shattuck-Eidens, R. Eeles, Q. Liu, N.A. Gruis, W. Ding, et al., Analysis of the p16 gene (CDKN2) as a candidate for the chromosome 9p melanoma susceptibility locus. *Nature Genetics*, 1994. **8**(1): p. 22-26.
7. Hussussian, C.J., J.P. Struewing, A.M. Goldstein, P.A.T. Higgins, D.S. Ally, M.D. Sheahan, et al., Germline p16 mutations in familial melanoma. *Nature Genetics*, 1994. **8**(1): p. 15-21.
8. Gruis, N.A., P.A. van der Velden, L.A. Sandkuijl, D.E. Prins, J. Weaver-Feldhaus, A. Kamb, et al., Homozygotes for CDKN2 (p16) germline mutation in Dutch familial melanoma kindreds. *Nat Genet*, 1995. **10**: p. 351.
9. Zuo, L., J. Weger, Q. Yang, A.M. Goldstein, M.A. Tucker, G.J. Walker, et al., Germline mutations in the p16INK4a binding domain of CDK4 in familial melanoma. *Nature Genetics*, 1996. **12**: p. 97.
10. Wiesner, T., I. Fried, P. Ulz, E. Stacher, H. Popper, R. Murali, et al., Toward an improved definition of the tumor spectrum associated with BAP1 germline mutations. *Journal of Clinical Oncology*, 2012. **30**(32): p. e337-40.
11. Jensen, D.E., M. Proctor, S.T. Marquis, H.P. Gardner, S.I. Ha, L.A. Chodosh, et al., BAP1: a novel ubiquitin hydrolase which binds to the BRCA1 RING finger and enhances BRCA1-mediated cell growth suppression. *Oncogene*, 1998. **16**(9): p. 1097-112.
12. Testa, J.R., M. Cheung, J. Pei, J.E. Below, Y. Tan, E. Sementino, et al., Germline BAP1 mutations predispose to malignant mesothelioma. *Nature Genetics*, 2011. **43**(10): p. 1022-5.
13. Abdel-Rahman, M.H., R. Pilarski, C.M. Cebulla, J.B. Massengill, B.N. Christopher, G. Boru, et al., Germline BAP1 mutation predisposes to uveal melanoma, lung adenocarcinoma, meningioma, and other cancers. *Journal of Medical Genetics*, 2011. **48**(12): p. 856-9.
14. Bertolotto, C., F. Lesueur, S. Giuliano, T. Strub, M. de Lichy, K. Bille, et al., A SUMOylation-defective MITF germline mutation predisposes to melanoma and renal carcinoma. *Nature*, 2011. **480**: p. 94.
15. Yokoyama, S., S.L. Woods, G.M. Boyle, L.G. Aoude, S. MacGregor, V. Zismann, et al., A novel recurrent mutation in MITF predisposes to familial and sporadic melanoma. *Nature*, 2011. **480**: p. 99.
16. Horn, S., A. Figl, P.S. Rachakonda, C. Fischer, A. Sucker, A. Gast, et al., TERT promoter mutations in familial and sporadic melanoma. *Science*, 2013. **339**(6122): p. 959-61.
17. Robles-Espinoza, C.D., M. Harland, A.J. Ramsay, L.G. Aoude, V. Quesada, Z. Ding, et al., POT1 loss-of-function variants predispose to familial melanoma. *Nature Genetics*, 2014. **46**(5): p. 478-481.
18. Aoude, L.G., A.L. Pritchard, C.D. Robles-Espinoza, K. Wadt, M. Harland, J. Choi, et al., Nonsense mutations in the shelterin complex genes ACD and TERF2IP in familial melanoma. *Journal of the National Cancer Institute*, 2015. **107**(2).
19. Teerlink, C.C., C. Huff, J. Stevens, Y. Yu, S.L. Holmen, M.R. Silvis, et al., A Nonsynonymous Variant in the GOLM1 Gene in Cutaneous Malignant Melanoma. *Journal of the National Cancer Institute*, 2018. **110**(12): p. 1380-1385.

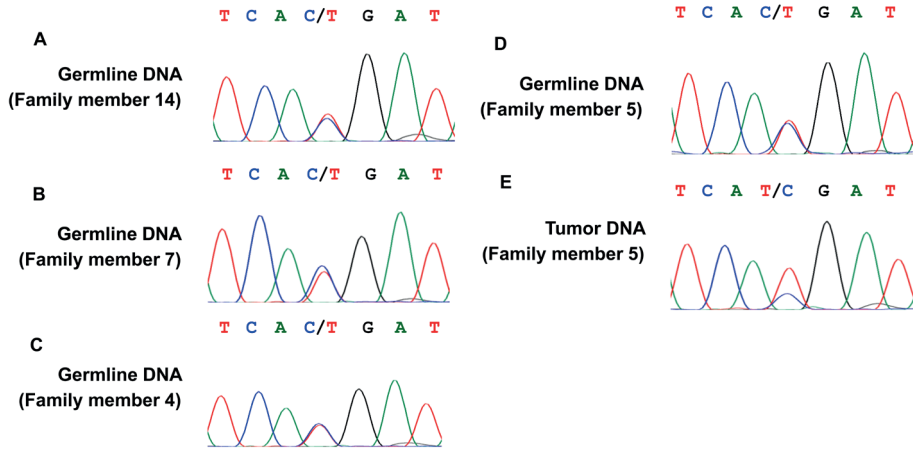
20. Artomov, M., A.J. Stratigos, I. Kim, R. Kumar, M. Lauss, B.Y. Reddy, et al., Rare Variant, Gene-Based Association Study of Hereditary Melanoma Using Whole-Exome Sequencing. *Journal of the National Cancer Institute*, 2017. **109**(12).
21. Aoude, L.G., E. Heitzer, P. Johansson, M. Gartside, K. Wadt, A.L. Pritchard, et al., POLE mutations in families predisposed to cutaneous melanoma. *Familial Cancer*, 2015. **14**(4): p. 621-628.
22. Read, J., K.A. Wadt, and N.K. Hayward, Melanoma genetics. *Journal of Medical Genetics*, 2016. **53**(1): p. 1-14.
23. Visser, M., N. van der Stoep, and N. Gruis, Progress report on the major clinical advances in patient-oriented research into familial melanoma (2013-2018). *Familial Cancer*, 2019.
24. Glusman, G., J. Caballero, D.E. Mauldin, L. Hood, and J.C. Roach, Kaviar: an accessible system for testing SNV novelty. *Bioinformatics* 2011. **27**(22): p. 3216-3217.
25. Pritchard, A.L., P.A. Johansson, V. Nathan, M. Howlie, J. Symmons, J.M. Palmer, et al., Germline mutations in candidate predisposition genes in individuals with cutaneous melanoma and at least two independent additional primary cancers. *PLoS One*, 2018. **13**(4): p. e0194098.
26. Versluis, M., M.J. de Lange, S.I. van Pelt, C.A. Ruivenkamp, W.G. Kroes, J. Cao, et al., Digital PCR validates 8q dosage as prognostic tool in uveal melanoma. *PLoS One*, 2015. **10**(3): p. e0116371.
27. Sabir, S.R., N.K. Sahota, G.D. Jones, and A.M. Fry, Loss of Nek11 Prevents G2/M Arrest and Promotes Cell Death in HCT116 Colorectal Cancer Cells Exposed to Therapeutic DNA Damaging Agents. *PLoS One*, 2015. **10**(10): p. e0140975.
28. Carlotti, F., M. Bazuine, T. Kekalainen, J. Seppen, P. Pognonec, J.A. Maassen, et al., Lentiviral vectors efficiently transduce quiescent mature 3T3-L1 adipocytes. *Molecular Therapies*, 2004. **9**(2): p. 209-17.
29. Heijkants, R.C., M. Nieveen, K.C. Hart, A. Teunisse, and A.G. Jochemsen, Targeting MDMX and PKCdelta to improve current uveal melanoma therapeutic strategies. *Oncogenesis*, 2018. **7**(3): p. 33.
30. Lek, M., K.J. Karczewski, E.V. Minikel, K.E. Samocha, E. Banks, T. Fennell, et al., Analysis of protein-coding genetic variation in 60,706 humans. *Nature*, 2016. **536**: p. 285.
31. Zerbino, D.R., P. Achuthan, W. Akanni, M.R. Amode, D. Barrell, J. Bhai, et al., Ensembl 2018. *Nucleic Acids Research*, 2018. **46**(D1): p. D754-d761.
32. Meirelles, G.V., A.M. Perez, E.E. de Souza, F.L. Basei, P.F. Papa, T.D. Melo Hanchuk, et al., "Stop Ne(c)king around": How interactomics contributes to functionally characterize Nek family kinases. *World Journal of Biological Chemistry*, 2014. **5**(2): p. 141-60.
33. Tate, J.G., S. Bamford, H.C. Jubb, Z. Sondka, D.M. Beare, N. Bindal, et al., COSMIC: the Catalogue Of Somatic Mutations In Cancer. *Nucleic Acids Research*, 2019. **47**(D1): p. D941-d947.
34. Rhodes, D.R., J. Yu, K. Shanker, N. Deshpande, R. Varambally, D. Ghosh, et al., ONCOMINE: a cancer microarray database and integrated data-mining platform. *Neoplasia* 2004. **6**(1): p. 1-6.
35. Chandrashekar, D.S., B. Bashel, S.A.H. Balasubramanya, C.J. Creighton, I. Ponce-Rodriguez, B. Chakravarthi, et al., UALCAN: A Portal for Facilitating Tumor Subgroup Gene Expression and Survival Analyses. *Neoplasia*, 2017. **19**(8): p. 649-658.
36. Hindson, C.M., J.R. Chevillet, H.A. Briggs, E.N. Gallichotte, I.K. Ruf, B.J. Hindson, et al., Absolute quantification by droplet digital PCR versus analog real-time PCR. *Nature Methods*, 2013. **10**(10): p. 1003-5.
37. Noguchi, K., H. Fukazawa, Y. Murakami, and Y. Uehara, Nek11, a new member of the NIMA family of kinases, involved in DNA replication and genotoxic stress responses. *Journal of Biological Chemistry*, 2002. **277**(42): p. 39655-65.
38. Melixetian, M., D.K. Klein, C.S. Sorensen, and K. Helin, NEK11 regulates CDC25A degradation and the IR-induced G2/M checkpoint. *Nature Cell Biology*, 2009. **11**(10): p. 1247-53.
39. Fry, A.M., L. O'Regan, S.R. Sabir, and R. Bayliss, Cell cycle regulation by the NEK family of protein kinases. *Journal of Cell Science*, 2012. **125**(Pt 19): p. 4423-33.
40. Sorensen, C.S., M. Melixetian, D.K. Klein, and K. Helin, NEK11: linking CHK1 and CDC25A in DNA damage checkpoint signaling. *Cell Cycle*, 2010. **9**(3): p. 450-5.
41. Liu, X., Y. Gao, Y. Lu, J. Zhang, L. Li, and F. Yin, Downregulation of NEK11 is associated with drug resistance in ovarian cancer. *International Journal of Oncology*, 2014. **45**(3): p. 1266-74.

42. Cerami, E., J. Gao, U. Dogrusoz, B.E. Gross, S.O. Sumer, B.A. Aksoy, et al., The cBio cancer genomics portal: an open platform for exploring multidimensional cancer genomics data. *Cancer Discoveries*, 2012. **2**(5): p. 401-4.
43. Gao, J., B.A. Aksoy, U. Dogrusoz, G. Dresdner, B. Gross, S.O. Sumer, et al., Integrative analysis of complex cancer genomics and clinical profiles using the cBioPortal. *Science Signaling*, 2013. **6**(269): p. pl1.
44. Chandrashekar, D.S., B. Bashel, S.A.H. Balasubramanya, C.J. Creighton, I. Ponce-Rodriguez, B.V.S.K. Chakravarthi, et al., UALCAN: A Portal for Facilitating Tumor Subgroup Gene Expression and Survival Analyses. *Neoplasia* 2017. **19**(8): p. 649-658.
45. Noguchi, K., H. Fukazawa, Y. Murakami, and Y. Uehara, Nucleolar Nek11 is a novel target of Nek2A in G1/S-arrested cells. *Journal of Biological Chemistry*, 2004. **279**(31): p. 32716-27.
46. Sherry, S.T., M.H. Ward, M. Kholodov, J. Baker, L. Phan, E.M. Smigielski, et al., dbSNP: the NCBI database of genetic variation. *Nucleic Acids Research*, 2001. **29**(1): p. 308-11.
47. Boomsma, D.I., C. Wijmenga, E.P. Slagboom, M.A. Swertz, L.C. Karssen, A. Abdellaoui, et al., The Genome of the Netherlands: design, and project goals. *European Journal of Human Genetics*, 2013. **22**: p. 221.
48. DeBoever, C., Y. Tanigawa, M.E. Lindholm, G. McInnes, A. Lavertu, E. Ingelsson, et al., Medical relevance of protein-truncating variants across 337,205 individuals in the UK Biobank study. *Nature Communications*, 2018. **9**(1): p. 1612.
49. Rahman, N., Realizing the promise of cancer predisposition genes. *Nature*, 2014. **505**(7483): p. 302-8.
50. Potjer, T.P., S. Bollen, A. Grimbergen, R. van Doorn, N.A. Gruis, C.J. van Asperen, et al., Multi-gene panel sequencing of established and candidate melanoma susceptibility genes in a large cohort of Dutch non-CDKN2A/CDK4 melanoma families. *International Journal of Cancer*, 2018.

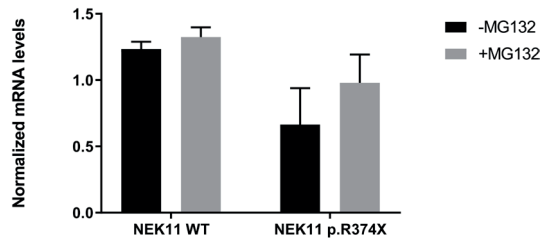
## SUPPLEMENTAL MATERIAL

Supplemental Table 1 Sequences of primer combinations

Primer Name	Sequence 5'-3'
NEK11-seq_exon12long_F	TGCACCACATTCACCTTGAT
NEK11-seq_exon12long_R	ATGCATTCAGTGCCAATTCA
NEK11-seq_exon12_F	CCAGTCAGTCTGTTGAAATAAGGA
NEK11-seq_exon12_R	TGTTTTCTCCCTTGTCCTTT
MNEK11_2F	GAAGAAAATAGCAAATGAATGCAAGAATTGAG
MNEK11_2R	CTCAATTCCTGCATTCATTGCTATTTCTTC
NEK11_exon3-4_F	CAAGAAAGCCAAACGAGGAG
NEK11_exon3-4_R	CCAGCTTGAGAGGAGTTGG
NEK11_ex2-3_F	AGCCAAACGAGGAGAGGAA
NEK11_ex2-3_R	CATTGGATTAGTTCTCCAACA
NEK11_L_ex17-18_F	CCCAGGACCACCAATTTTC
NEK11_L_ex17-18_R	GAGTAGGTTCTTTCCCATCGT
NEK11_exon11-13_inclMT_short_F	GAAAGCCAGGAAGCTGAAAA
NEK11_exon11-13_inclMT_short_R	TTGCTCCTCTTTTCTTCCA
NEK11_exon11-12_inclMT_short_F	GAGAAAGCCAGGAAGCTGAA
NEK11_exon11-12_inclMT_short_R	AGCTGCTGAAAGTTCCGAGA
NEO_F	ATTCGGCTATGACTGGGCAC
NEO_R	TTCAGTGACAACGTCGAGCA
TomatoRed_F	TTCATGTACGGCTCCAAGGC
TomatoRed_R	TTGTAGATCAGCGTGCCGTC
CAPNS1_F	ATGGTTTTGGCATTGACACATG
CAPNS1_R	GCTTGCCTGTGGGTCCG
SRPR_F	CATTGCTTTTGACGTAACCAA
SRPR_R	ATTGCTTGCATGCGGCC
NEK11_SNP_rs4974475_F	GAGACAGAAAGAACCCTGAACACA
NEK11_SNP_rs4974475_R	CTGCTCACAATGTACTTTCATGGA
dPCR assay ID (WT/R374X)	TCTACATTCACCTTTAAATTTACAGAAAGATTGTGGAAGAAAAATATG
dHsaMDS101412638	AAGAAAATAGCAAA[C/T]GAATGCAAGAATTGAGATCTCGGAACCTT TCAGCAGCTGAGTGTGATGTACTCCATGTAAG

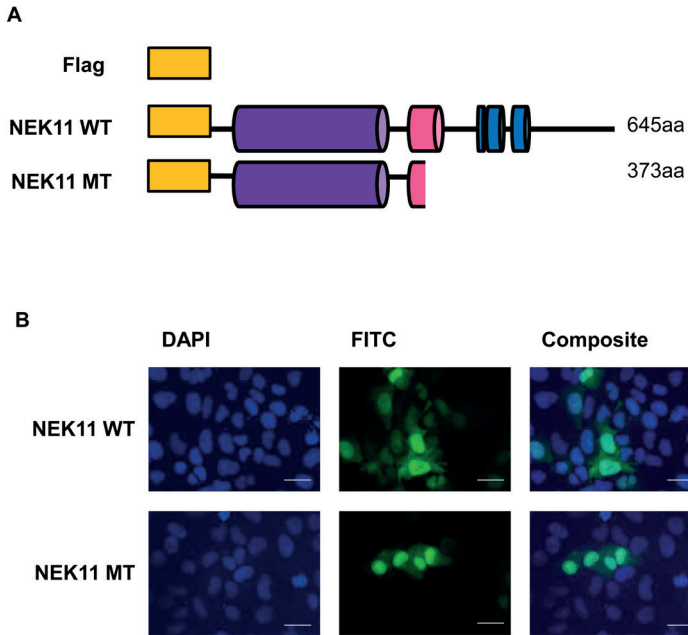


**Supplemental Figure 1 Genotyping of a common SNP (rs4974475) in a Dutch melanoma family.** Chromatogram showing DNA sequence and variant presence [T] in germline DNA of **A)** healthy family member 14 and in germline DNA of *NEK11* p.Arg374Ter mutation carriers **B)** family member 7, **C)** family member 4 and **D)** family member 5. **E)** Loss of the normal allele [C] was detected in tumor DNA of family member 5.



**Supplemental Figure 2 Relative mRNA expression data in transiently transfected U2OS cells.** Relative mRNA levels normalized to *CAPNS1* and *SRPR* reference genes and subsequently corrected to Tomato Red to correct for transfection efficiency. Data shown represent mean expression from 3 independent experiments. Error bars show Standard Error of the Mean (SEM). Statistical significance is shown as \* $p < 0.05$ , \*\* $p < 0.005$ , \*\*\* $p < 0.0005$ .





**Supplemental Figure 3 Subcellular localization of NEK11 wildtype and p.Arg374Ter proteins.** **A)** Schematic representation of Flag-tagged NEK11 expression vectors, with the wildtype (WT) construct consisting of 645 amino acids. In purple the N-terminal catalytic domain is shown, in pink is the coiled-coil domain and in blue the C-terminal PEST-like domain. Following site-directed mutagenesis the resulting NEK11 p.Arg374Ter (MT) protein consists 373 amino acids, with the whole C-terminal PEST-like domain and part of coiled-coil domain is lost [27] **B)** Immunofluorescence staining of NEK11 WT and NEK11 MT protein localization in U2OS cells (scale bars represent 10  $\mu$ m).

